Original Article

SHM Structural Health Monitoring

Structural Health Monitoring
2014, Vol. 13(6) 644–659

DOI: 10.1177/1475921714556568
shm.sagepub.com
SAGE

Structural health monitoring of offshore wind turbines using automated operational modal analysis

Christof Devriendt[1], Filipe Magalhães[2], Wout Weijtjens[1], Gert De Sitter[1], Álvaro Cunha[2] and Patrick Guillaume[1]

Abstract

This article will present and discuss the approach and the first results of a long-term dynamic monitoring campaign on an offshore wind turbine in the Belgian North Sea. It focuses on the vibration levels and modal parameters of the fundamental modes of the support structure. These parameters are crucial to minimize the operation and maintenance costs and to extend the lifetime of offshore wind turbine structure and mechanical systems. In order to perform a proper continuous monitoring during operation, a fast and reliable solution, applicable on an industrial scale, has been developed. It will be shown that the use of appropriate vibration measurement equipment together with state-of-the art operational modal analysis techniques can provide accurate estimates of natural frequencies, damping ratios, and mode shapes of offshore wind turbines. The identification methods have been automated and their reliability has been improved, so that the system can track small changes in the dynamic behavior of offshore wind turbines. The advanced modal analysis tools used in this application include the poly-reference least squares complex frequency-domain estimator, commercially known as PolyMAX, and the covariance-driven stochastic subspace identification method. The implemented processing strategy will be demonstrated on data continuously collected during 2 weeks, while the wind turbine was idling or parked.

Keywords

Monitoring, offshore wind turbine, operational modal analysis, automated, signal processing

Introduction

Online monitoring of wind turbines is a more and more critical issue as the machines are growing in size and offshore installations are becoming more common. To decrease the power generation cost by optimizing the weight, the turbines are becoming structurally more flexible and therefore are more affected by the wind and wave excitation. Thus, an accurate validation of their dynamic behavior is mandatory. On the other hand, inspection and maintenance of offshore installations are much more cumbersome and expensive than the inspection and maintenance of onshore turbines. Thus, a remote monitoring application with the ability to predict structural changes can help to reduce operation and maintenance (O&M) costs and contributes to a better assessment of the lifetime of these structures.

Many large-scale offshore wind farm projects use monopile foundations to obtain a cost-effective design. Even for water depths beyond 30 m, the monopile design is currently being considered as an option. During the design of these monopile structures, fatigue due to combined wind and wave loading is one of the most important problems to take into account. Structural resonances that are excited by the dynamic wind and wave forces can lead to large amplitude stresses and subsequent accelerated fatigue. The current practice is to design the wind turbine support structure in such a way that the tower fundamental resonance does not coincide with the fundamental rotational (1P) and blade passing (3P for three-bladed turbines)

[1]Acoustics and Vibration Research Group, Vrije Universiteit Brussel, Brussels, Belgium
[2]ViBest, Faculty of Engineering, University of Porto, Porto, Portugal

Corresponding author:
Christof Devriendt, Acoustics and Vibration Research Group, Vrije Universiteit Brussel, Pleinlaan 2 B, B-1050 Elsene, Brussels, Belgium.
Email: christof.devriendt@vub.ac.be

frequencies of the rotor.[1] However, the higher order rotor harmonics might still coincide with higher modes of the support structure inducing important vibrations and consequently reducing the fatigue-life. Experiments performed by the Maritime Research Institute Netherlands (MARIN) also confirmed that breaking waves could induce significant oscillations and accelerations in the turbine.[2] This can have a significant effect on the lifetime of the wind turbines.

In the particular case of monopile foundations, scouring and reduction in foundation integrity over time can be problematic. These issues reduce the fundamental structural resonances of the support structure. As a consequence, the first resonance can be shifted to the frequency range in which much of the broadband wave and gust energy is concentrated. Thus, a lower natural frequency means that more energy can create resonant behavior increasing fatigue damage.[1] On the other hand, it might also affect the higher modes of the support structure making them coincide with some of the higher order rotor harmonics, for example, 6P, 9P. Numerical analysis has shown that the natural frequencies are notably affected by scour. In Zaaijer,[3] a study of the dynamic behavior for a tripod and monopile design of a 6-MW turbine is presented. It is shown that the natural frequencies of the support structure decrease when scour occurs. This effect is more important for the second resonance frequency of the support structure, which, in the case of monopoles foundations, presents a decrease of 10% for a scour depth of 5 m (length approximately equal to the assumed pile diameter). Continuous monitoring of the effect of scour on the dynamics of the wind turbine will therefore help to make a better decision on when to plan maintenance activities on the scour protection.

In this context, the development and validation of tools for automatic identification of the modal parameters based on the measurement of the dynamic response of wind turbines is fundamental. The success of subsequent structural health monitoring algorithms depends on the accuracy of these identified parameters.

Description of the dynamic monitoring system

First, it should be stated that the main goals of the monitoring system described in this section are the characterization of the wind turbine tower vibrations and the tracking of the structure most relevant modal parameters, in order to evaluate its structural performance and detect eventual abnormal behaviors that may reduce its lifetime and or may imply maintenance activities.

The monitoring campaign is performed at the Belwind wind farm, which consists of 55 Vestas V90 3 MW wind turbines. The wind farm is located in the North Sea on the Bligh Bank, 46 km off the Belgian coast (Figure 1).

The instrumented wind turbine is placed on a monopile foundation structure with a diameter of 5 m and a wall thickness of 7 cm. The hub height of the wind turbine is on average 72 m above sea level. The transition piece is 25 m high. The interface level between the transition piece and the wind turbine tower is at 17 m above sea level. The actual water depth at the location of the tested wind turbine is 22.9 m and the monopile has a penetration depth of 20.6 m. The soil is considered stiff and mainly consists of sand.

The structural components instrumented in this campaign are the tower and the transition piece. Measurements are taken at four levels using a total of 10 sensors. The measurement locations are indicated in Figure 2. The chosen levels are 67, 37, 23, and 15 m above sea level, respectively, levels 1–4. There are two accelerometers mounted at the lower three levels and four at the top level. The chosen configuration is primarily aimed at identification of tower bending modes. The two extra sensors on the top level are placed to capture the tower torsion. The data acquisition system, a CompactRIO system of National Instruments, is mounted in the transition piece. Since the project aims at characterizing the dynamics during a long period, it was also required that the data acquisition system can be remotely accessed and is capable of automatic startup in case of power shutdowns. The data acquisition software allows the continuous recording of accelerations. The selected accelerometers have a high sensitivity (1 V/g) and are able to measure very low-frequency signals (0–250 Hz). This is necessary considering that the lower modal frequencies of interest are expected to be around 0.35 Hz, and the expected vibration magnitude is very low.

The monitoring software records the measured acceleration with a sampling frequency of 20 Hz and creates consecutive data files with a duration of 10 min, which are then sent to a server installed onshore using a dedicated fiber installed under the seabed. Therefore, in each day, a total of 144 files are created. These data files receive a time-stamp in order to be possible to correlate the parameters derived from the acceleration time series with the SCADA and ambient data. The SCADA data (power, rotor speed, pitch angle, nacelle direction) and ambient data (wind speed, wind direction, wave height, wave period, temperature, etc.) are collected at 10-min intervals. Figure 2 characterizes the SCADA data collected during the monitoring period under analysis in this work. Note that the x-axis is labeled as "index" and each data point represents a 10-min value; since the

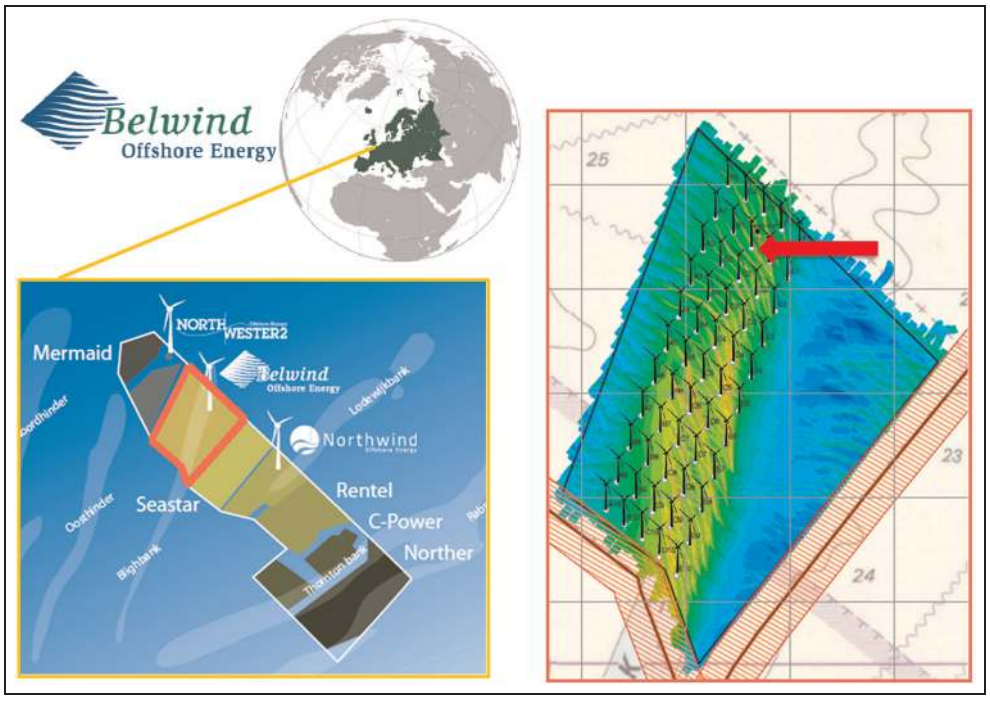

Figure 1. Location Belwind wind farm (left), park layout (right) and wind turbine location (arrow).

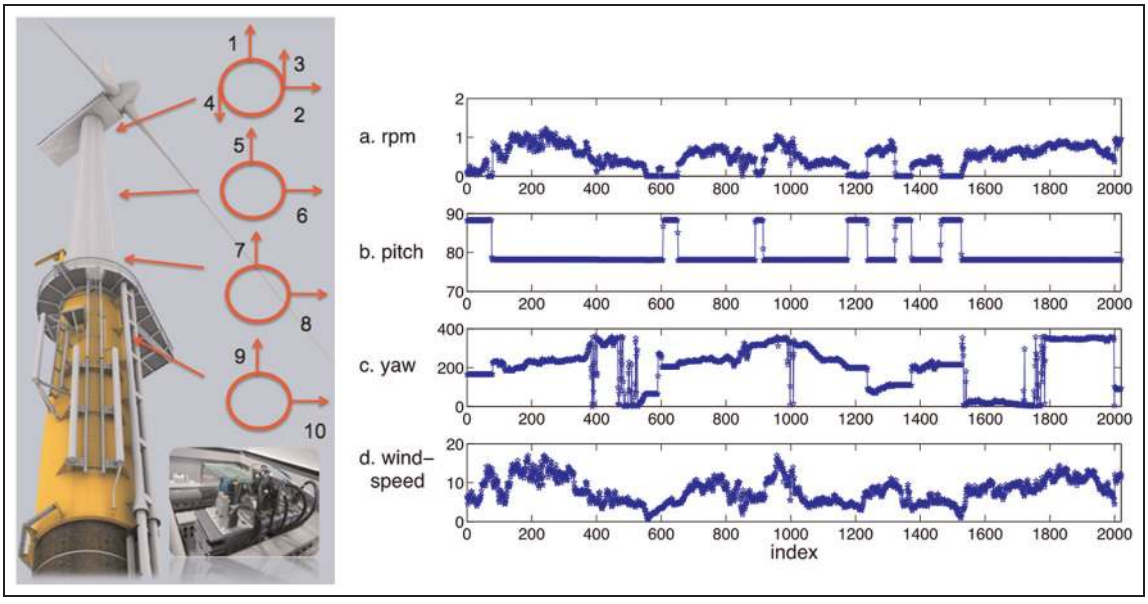

Figure 2. Measurement locations and data acquisition system based on NI CompactRIO System (left), SCADA data (right): from top to down: r/min, pitch angle (°), yaw angle (°), and wind speed (m/s).

monitoring period has a duration of 2 weeks, a total of 2016 values are presented. The wind speed is varied between 0 and 16 m/s. The pitch angle was almost constant during the period of analysis, with a pitch angle of 78° or 88.3°. Most of the time, the wind turbine was idling with a rotational speed lower than 1.3 r/min or was in parked conditions.

As already referred, during the long-term measurement campaign, our aim is to continuously monitor the vibration levels and the evolution of the frequencies and damping values of the fundamental modes of the tower and foundation. In order to fulfill this goal, the following steps will be followed:

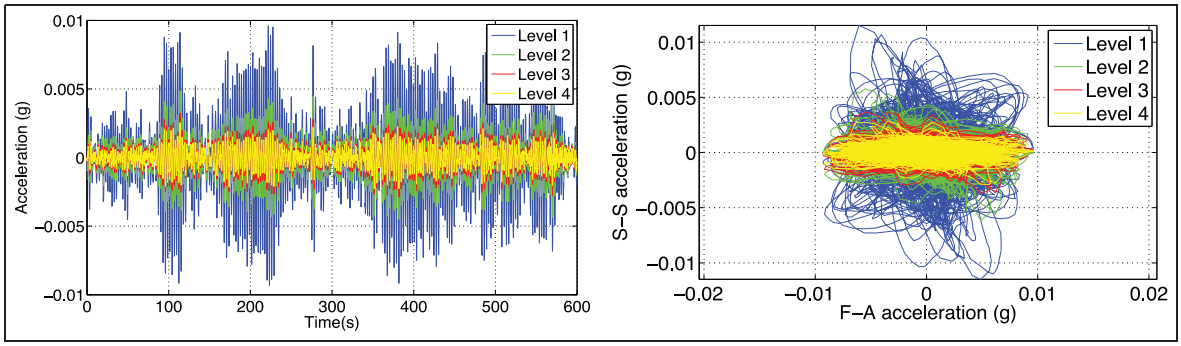

Figure 3. Example of measured accelerations during ambient excitation on four levels, with level 1 the highest level: left plot—accelerations along the side–side direction; right plot—movement seen from above.

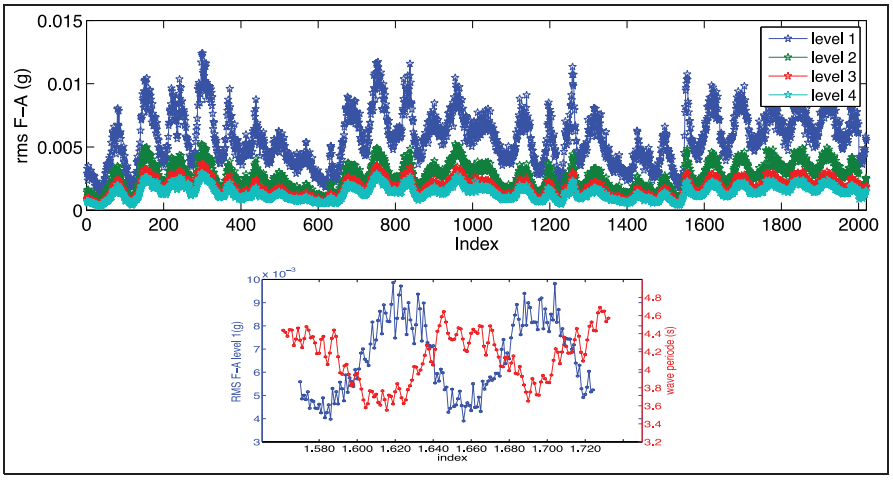

Figure 4. RMS values of the acceleration time series in the FA-direction during monitoring period (top), the variation during 24 h of the RMS values of the accelerations in the FA-direction at the highest level (blue) and the wave period (red) (bottom).
RMS: root mean square; FA: fore-aft.

Step 1. Pre-processing of vibration data.
Step 2. Automated operational modal analysis (OMA).
Step 3. Tracking mode shapes, frequencies, damping values.

In the following sections, the algorithms associated with these steps will be discussed in detail. Then, in section "Monitoring results," their performance will be demonstrated on 2 weeks of data.

Pre-processing of vibration data (Step 1)

The inputs for the following steps are the time series measured by the 10 accelerometers. Each day the successive 10-min data blocks are processed, resulting in 144 values per day per calculated parameter. Considering the frequency band of interest and in order to reduce the amount of data, the recorded time series have been filtered with a band-pass filter and re-sampled with a sampling frequency of 12.5 Hz.

Since the accelerometers are mounted on the wind turbine tower and in the transition piece, in order to measure the vibrations along the axis of the nacelle, it is necessary to take the yaw angle (angle of the nacelle with regard to a fix coordinate system) into account and project the measured directions into the coordinate system of the nacelle.[4] Figure 3 shows an example of the accelerations measured on the four levels for 10 min of wind and wave excitation. It also shows the movement seen from above in both the fore-aft (FA—along the axis of the nacelle) and side–side (SS—perpendicular to the axis of the nacelle) directions.

Figure 4 presents one of the plots, created in the first step of the continuous monitoring routines. The plot shows the root mean square (RMS) values of the acceleration time series in the FA-direction for each 10-min

interval. This figure already shows some of the dynamic characteristics of an offshore wind turbine. The operational deflection shape of the wind turbine in parked conditions results in a maximum vibration amplitude at the upper level and a minimum vibration amplitude at the lowest level.

It can also be observed that the RMS values vary periodically. This is due to the changing wave periods, which vary accordingly between 3 s (0.333 Hz) and 6 s (0.166 Hz), respectively, getting closer and further away from the resonance frequencies of the fundamental first bending modes of the wind turbine, which are located around 0.35 Hz. Figure 4 also compares the evolution of the wave period and RMS values of the accelerations at the highest level in the FA-direction during 1 day. One can conclude that waves have the possibility to excite the structure into dynamically amplified vibrations when the wave period gets closer to the fundamental foundation/tower frequencies. This also confirms the relevance to monitor these frequencies. Note that the RMS values are also affected by other ambient parameters such as wave height and wind speed.

Automated OMA (Step 2)

Introduction

Identification of the modal parameters of a full-scale operating wind turbine is particularly difficult, and in the research community, a lot of effort still goes into the development of suitable methods to tackle this problem.[5] Classical experimental modal analysis methods cannot be applied because the input force due to the wind and the waves cannot be measured. For this reason, OMA methods have to be used to identify the modal parameters from the response of a mechanical structure in operation subjected to unknown random perturbations.[6–10]

These methods work under the assumption that the system is linear time-invariant during the analyzed time interval. Moreover, they assume that the unknown input excitation is white noise within the frequency band of interest. However, due to the rotating rotor and the corresponding harmonic force contributions, the white noise assumption is violated. As a consequence, the application of OMA becomes more challenging. The analysis in this article is focused on a period during which the wind turbine was idling or in parked conditions, presenting a rotating speed always lower than 1.5 r/min. This means that the risk of having some harmonic components in the frequency band of interest resulting from the rotating equipment is very low. Therefore, the white noise assumption in parked conditions is valid and OMA is applicable.

In the context of dynamic monitoring systems recording continuously the responses of an instrumented structure, it is very important to develop tools that can process the collected data automatically. Consequently, a lot of research has been developed with the goal of achieving algorithms that can automatically extract accurate estimates of modal parameters from continuously recorded structural responses during normal operation conditions.

The research efforts that have been performed to automate the identification of structural modal parameters using parametric algorithms are focused on three complementary aspects: the development of new identification algorithms that can produce clearer stabilization diagrams (Cauberghe et al.[11]), the study of criteria to characterize the quality of the estimates and finally the development of tools to automatically interpret stabilization diagrams.

In the field of the development of new identification algorithms, an important outcome was the poly-reference least squares complex frequency-domain estimator (p-LSCF) method,[12] which provides clearer stabilization diagrams that facilitate the selection of the physical mode estimates.[11]

Concerning the definition of additional criteria to distinguish physical mode estimates from spurious ones, such as the complexity of the modal vector, the modal transfer norm or uncertainty of the estimates, details can be found in Verboven et al.[13] and Reynders et al.[14]

After the elimination of all, or at least part of the spurious mode estimates, there is still the need for a procedure to group all the estimates associated with models of different orders that are related with the same physical mode. The most simplistic approaches overcome this step with the selection of a conservative model order, instead of analyzing the results of several model orders. However, this is not the most adequate procedure, because it can happen that the selected model does not contain estimates for all the modes and even if all estimates are present, there is no guarantee that the estimates provided by that model order are the best ones. A natural way for the automatic interpretation of stabilization diagrams consists in the development of algorithms to mimic the decisions that an experienced modal analyst takes during the examination of a stabilization diagram. This is followed for instance in Scionti et al.[15]

An alternative is the use of cluster analysis.[16] This can be performed using non-hierarchical clustering algorithms, as it is presented in Verboven et al.,[13] Goethals et al.[17] and Carden and Brownjohn;[18] or using hierarchical algorithms, as it is described in Magalhães et al.[19] and Verboven et al.[20]

Description of the implemented procedure

In order to allow a proper structural health monitoring during operation, based on the dynamic properties of the wind turbine foundation and tower, a fast and reliable solution applicable on industrial scale has been developed. The identification methods have been automated, and their reliability for this particular type of data has been improved.

In Verboven et al.[13] and Vanlanduit et al.,[21] automated modal identification approaches are presented based on the use of a frequency-domain maximum likelihood estimator (MLE) and stochastic validation criteria combined with a fuzzy C-means clustering approach, yielding promising results. In Magalhães et al.,[19] the authors developed a methodology for automatic identification of modal parameters, using parametric identification methods, based on a hierarchical clustering algorithm. This has been successfully applied in the continuous monitoring of a bridge. In this work, the algorithm adopted to automate the identification process is a combination of the above approaches and consists of the following three steps:

Step 2.1. Identification of modal parameters using a state-of-the-art OMA estimator.
Step 2.2. Perform a hierarchical clustering algorithm on the identified poles.
Step 2.3. Classification and evaluation of the identified clusters using a fuzzy clustering algorithm.

Identification of modal parameters using a state-of-the-art OMA estimator. Identification of the modal parameters from the collected data sets can be achieved with different OMA techniques. A detailed description of some of these methods can be found in Hermans and Van Der Auweraer,[6] Brincker et al.,[7] Cauberghe,[8] and Peeters and De Roeck.[22] The techniques used in this article are the p-LSCF[12] and the covariance-driven stochastic subspace identification (SSI-COV) method.[22]

When the vibrations measured during normal operation are used, the first task consists of calculating the correlation functions of the measured accelerations. It has been shown that the output correlation of a dynamic system excited by white noise is proportional to its impulse response.[23] Therefore, the fast Fourier transformation of the positive time lags of the correlation functions can directly be used as input for the frequency-domain identification methods. The time-domain OMA estimators can be directly applied to a matrix with the auto- and cross-correlation functions. The parameters that need to be chosen are the length of the used time segment and the number of time lags taken from the correlation function used for the spectra calculation.[24] The spectra resolution, controlled by the number of time lags taken from the correlation functions, should be high enough to well characterize all the modes within the selected frequency band. At the same time, it should be kept as low as possible to reduce the effect of the noise. In El-Kafafy et al.[10] and Devriendt et al.,[25] different numbers of time lags taken from the correlation functions have been evaluated and 512 points taken from the correlation functions were found to be a good choice. In Devriendt et al.,[26] it was evaluated if 10 min for the length of the time segments used in the continuous monitoring of the offshore wind turbine would be sufficient to identify the modal parameters in a robust way. It is assumed that within a time segment of 10 min, the ambient conditions, for example, wind speeds, stay more or less constant, needed for the OMA time-invariant assumption. Ten minutes is also the commonly used time interval for the SCADA data and the Meteo data, and thus has the advantage of making future analyses of the data easier. It was found that although the standard deviation (SD) when using only 10 min was higher than for data sets using, for example, 40 min, especially for the damping values of the first FA and SS bending modes, the mean values were comparable, and thus 10 min were considered sufficient to find estimates of the modal parameters with acceptable quality.

Then, the poles are estimated with an OMA estimator for different model orders. In a non-automated way, these results can be used to construct a stabilization diagram from which the user can try to separate the physical poles (corresponding to modes of the system) from the mathematical ones.[11] By displaying the poles (on the frequency axis) for an increasing model order (i.e. number of modes in the model), the diagram helps to select the physical poles, since, in general, they tend to stabilize for an increasing model order, while the computational poles scatter around. As a result, a construction of the stabilization chart is nowadays one of the requirements for a modal parameter estimation algorithm, and it has become a common tool in modal analysis.

Figure 5 shows an example of a stabilization diagram using a 10-min time segment with 512 time lags taken from the correlation functions and a maximum model order of 60. The analysis focuses in the frequency range of 0–2 Hz, where the main vibration modes of interest are expected. The stabilization diagram seems to have around five well-identifiable stable poles. In a non-automated approach, we could manually select the poles in the stabilization diagram by clicking on the stable poles, indicated by a red "s." The results of such a manual selection can be found in Table 1. It is clear that this may depend on the user as the selection of different poles will give slightly different results. For high noise levels, the stabilization diagrams can be difficult to interpret and the results become even more user

Table 1. Frequencies and damping values of identified modes by manual selection and cluster analysis.

Manual selection										
Freq. (Hz)	0.3295	0.3576	0.3711	–	0.7387	1.0727	1.2033	–	1.4811	1.5692
Damp.	0.7267	0.9380	0.9290	–	2.1074	1.2333	0.9504	–	1.8778	0.9528
Cluster analysis										
Freq. (Hz)	0.3345	0.3578	0.3705	0.5133	0.7394	1.0725	1.2045	1.4304	1.4831	1.5679
Damp.	1.3608	0.9743	1.1210	1.5774	1.3097	1.1644	0.9880	0.4201	1.5843	0.8535

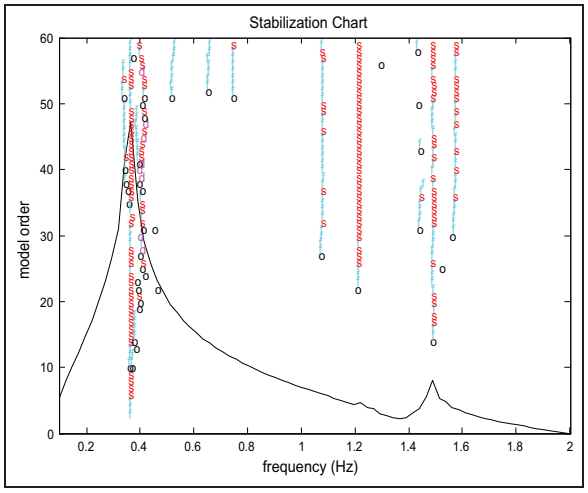

Figure 5. Stabilization diagrams for 10 min of data using the p-LSCF estimator.
p-LSCF: poly-reference least squares complex frequency-domain estimator.

dependent. Moreover, stabilization diagrams require interaction and therefore, they cannot directly be used when autonomous modal parameter estimation is needed. The next paragraph will present how this process can be automated in a robust way.

Perform a hierarchical clustering algorithm on the identified poles. For the automatic selection of the physical poles that represent the modes of interest, a hierarchical clustering algorithm is used. The goal is to cluster poles that are related to the same physical mode. Several basic procedures are available in the MATLAB Statistics Toolbox, and several articles have successfully applied these methods.[13,19,21] In this work, a robust agglomerative hierarchical approach was used based on the method presented in Verboven et al.[27] The algorithm starts with the calculation of a distance matrix between all the poles, estimated for the different orders. In order to make the cluster algorithm suited for the identification of the different system poles, the following conditions must be taken into account to assure that each structural mode is represented by just one cluster:

1. The number of poles in one cluster is limited to the selected maximum model order minus the number of orders that are not considered for clustering.
2. A pole is added to a cluster by taking the nearest pole that results from a solution corresponding to a different model order.
3. All the poles corresponding to a single physical pole must be clustered before a next cluster is started, while the poles already clustered are not further considered.

Each time a new cluster is initiated, a new distance matrix is computed using the remaining poles. When looking for a new pole to be added to a cluster, a predefined frequency interval (i.e. 1% of the mean frequency of the initiated cluster) is considered. In our case, it was possible to consider such a small interval from the start because of the high quality of the measurements and the corresponding estimates. When the noise levels of the collected data are higher, a larger interval can be used. As long as the number of poles, each corresponding to a different model order, is larger than the maximum number of poles that a cluster can contain, the width of the frequency interval is reduced. This maximum number of poles equals the maximum model order minus the number of orders that are not considered for clustering. One can choose not to use the first orders for the clustering algorithm, because the low-order estimates can be of less quality and because some system poles only show up as stable lines for higher model orders. One can also choose not to consider clusters with a small number of poles. Figure 6 shows the results of the algorithm when the first 30 orders were not used and only clusters with more than 20% of the maximum number of poles a cluster can contain were retained.

It could be observed in the stabilization diagram (Figure 5) that the poles are very scattered around the main peak, making the manual pole selection less obvious. However, looking at the results of the clustering algorithm, we can clearly see three clusters appearing (Figure 6 right) and we can easily identify the clusters for the first FA mode and the SS mode. Therefore, this

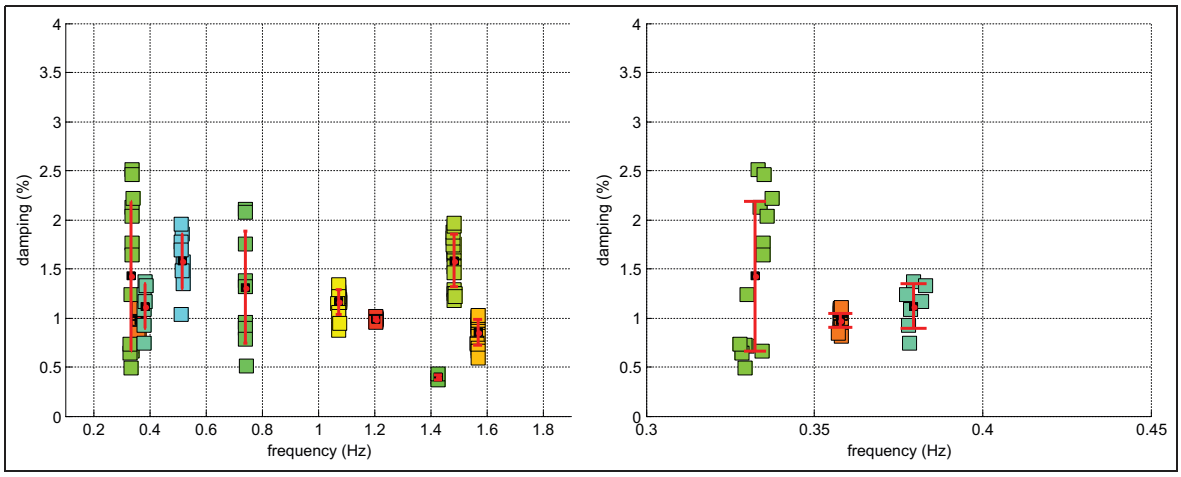

Figure 6. Clusters obtained when using the agglomerative hierarchical approach (left); zoom on clusters around first FA mode (right).
FA: fore-aft.

seems to be an efficient approach for the automatic identification. Based on the cluster results, a statistical analysis yields the mean and SD for each of the estimated poles and hence for the damped natural frequencies and damping ratios. In Table 1, the mean values are presented for comparison with the manual selection from the stabilization diagrams. The SD on the frequencies and damping values can be used for validation purposes and for the separation of physical and mathematical poles. One can also calculate an identification success rate by dividing the number of poles in each cluster by the maximum number of poles a cluster can contain. These parameters will be used in the next paragraph to distinguish the well-identified clusters from the clusters with estimates of less quality or to distinguish the physical poles from the mathematical ones. Note that mode information was not included in the cluster analysis. Other cluster algorithms include the modal assurance criterion (MAC)[28] when calculating the distance matrix.[19] The MAC value allows quantifying the degree of correlation between the mode shapes related with different poles. In this work, it was decided to base the clustering only on the poles (related with the natural frequencies and modal damping ratios), because useful mode information might not always be available; this might especially be the case when only a small number of sensors is used. If mode information is available, it will be used to distinguish physical from non-physical poles as will be discussed later in the next section.

Classification and evaluation of the identified clusters using a fuzzy clustering algorithm. The clustering procedure assures that each of the system poles will be represented by just one single cluster. However, since typically high model orders are chosen, not each cluster corresponds to a system pole. Therefore, each of the clusters needs to be assessed for its physicality. Second, when continuous monitoring is done not all data sets will allow to identify all the physical modes and their corresponding frequencies and damping values with high confidence. Therefore, criteria can be defined that can distinguish physical modes from mathematical ones and that allow to discard estimates of low quality. The number of poles in a cluster, or the identification success rate, as well as the SDs on the frequencies and damping values of each cluster, may give a good indication for the quality of the identified poles and their clusters. When a sufficient number of sensors is available, mode shape information can be used to further evaluate the clusters by also considering the well-known validation criteria such as the MACs, modal phase collinearity (MPC) and the modal phase deviation (MPD).[28] For each pole in a cluster, the corresponding mode shape information can be computed and the following percentage ratios can be calculated: the fraction of mode shapes that have an MPC larger than 80% and an MPD smaller than 10°.

An iterative fuzzy C-means clustering algorithm, proven to be useful for the automation of the modal mode extraction, can now be used to evaluate the clusters. In Verboven et al.[13] and Vanlanduit et al.,[21] the approach was used to classify the identified poles into physical and computational poles. Based on the results for each of the validation criteria, the clusters identified after the first step will now be grouped into two classes using this algorithm, that is, cluster with well-identified physical poles and clusters with computational poles or badly identified physical poles. This algorithm is

implemented in the MATLAB Fuzzy Logic Toolbox. The output of the fuzzy C-means clustering algorithm gives a classification result for the clusters. If the classification result is larger than 50%, then it is decided that the cluster belongs to the class of clusters with physical poles that have a good estimate and can be used for continuous monitoring. The following validation criteria will be used:

- Variable 1: the SDs of the estimated resonance frequencies;
- Variable 2: the SDs of the estimated damping values;
- Variable 3: the identification success rate;
- Variable 4: the fraction of mode shapes that have an MPC larger than 80%;
- Variable 5: the fraction of mode shapes with an MPD smaller than 10°.

Table 2 gives the values for these variables for all clusters obtained after the hierarchical clustering algorithm in case of the data set of 10 min under analysis and using 512 time lags for the correlation functions. Table 2 also gives the mean MAC, MPC, and MPD values within a cluster. After the variables have been computed, an interval scaling[27] is performed in order to obtain variables of the same type, which are defined in the same interval (e.g. 0–1). The variables with a large range (i.e. variables 1 and 2) are transformed using a logarithmic transform. Second, all variables are subtracted by their minimum and divided by their range (i.e. the maximum minus the minimum).

Figure 7 presents the results of the fuzzy clustering algorithm. In the first case, only variables 1 and 2 are used. As can be noticed, the SD gives a good distinction between the physical and mathematical clusters and those clusters that are not very well identified. In this case, the accepted clusters correspond with the well-excited modes in the FA-direction (see later in Figure 8). This also justifies the usefulness of the uncertainty values derived in the initial hierarchical clustering approach. When we include variable 3, we can see that more clusters are positively classified. There are seven clusters that stand out because of their high identification success rate (i.e. >80%), which correspond with the stable lines that were previously observed in the stabilization diagrams (Figure 5). The first cluster with a high identification success rate is, however, not accepted in the final classification results, due to its high SDs on damping and frequency. This cluster was related with the coloring due to the wave excitation. Finally, we can also evaluate the effect of variables 4 and 5. These variables enhanced the classification result of the last two clusters. These clusters are physical modes related with weakly excited higher bending

Table 2. Variables used for the fuzzy C-means clustering algorithm in case of the data set of 10 min and using 512 time lags and mean MAC, MPC, and MPD values within a cluster.

Freq. (Hz)	0.3345	0.3578	0.3705	0.5133	0.7394	1.0725	1.2045	1.4304	1.4831	1.5679
Damp. (%)	1.3608	0.9743	1.1210	1.5774	1.3097	1.1644	0.9880	0.4201	1.5843	0.8535
Variable 1	0.0086	1.5981 e − 004	0.0022	0.0034	9.9442 e − 004	0.0013	2.0600 e − 004	0.0056	0.0015	7.6754 e − 004
Variable 2	0.7734	0.0979	0.2237	0.2800	0.5719	0.1254	0.0155	0.0582	0.2653	0.1310
Variable 3	88.23	100	41.17	52.94	52.94	100	100	29.41	100	100
Variable 4	26.66	100	0	44.44	55.55	82.35	17.64	60	52.94	82.35
Variable 5	33.33	100	0	47.05	44.44	66.66	100	100	100	100
Mean MAC	0.8417	0.9999	0.9931	0.9773	0.9913	0.9985	0.9988	0.9945	0.9991	0.9994
Mean MPC	50.09	99.8364	5.1672	57.8099	63.1445	87.6287	52.7727	83.3488	71.542	86.609
Mean MPD	22.4980	0.4989	45.707	27.5538	18.5094	4.7630	4.9787	4.8635	3.5552	3.6429

MAC: modal assurance criterion; MPC: modal phase collinearity; MPD: modal phase deviation.

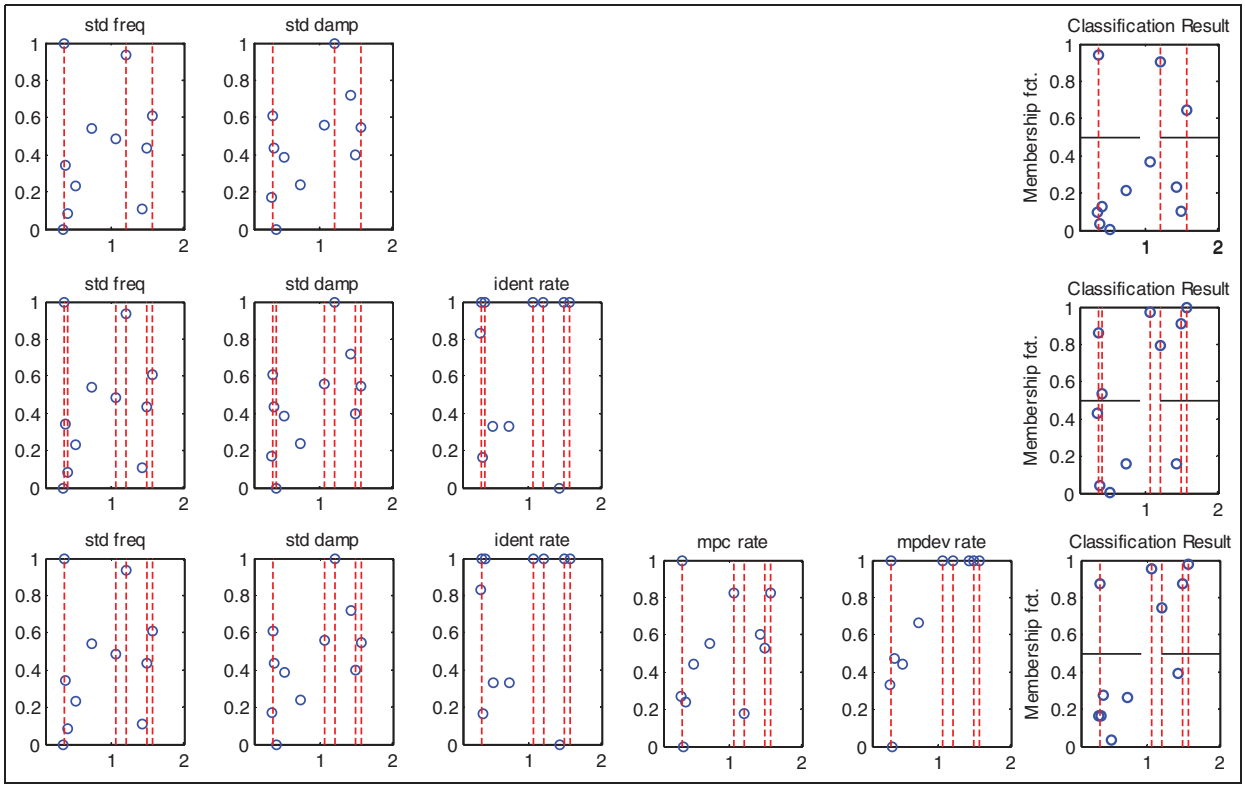

Figure 7. Variables used for the clustering algorithm in case of the data set of 10 min and using 512 time lags and the cluster classification results in case of using variables 1 and 2 (top); variables 1, 2, and 3 (middle) and using all five variables (bottom).

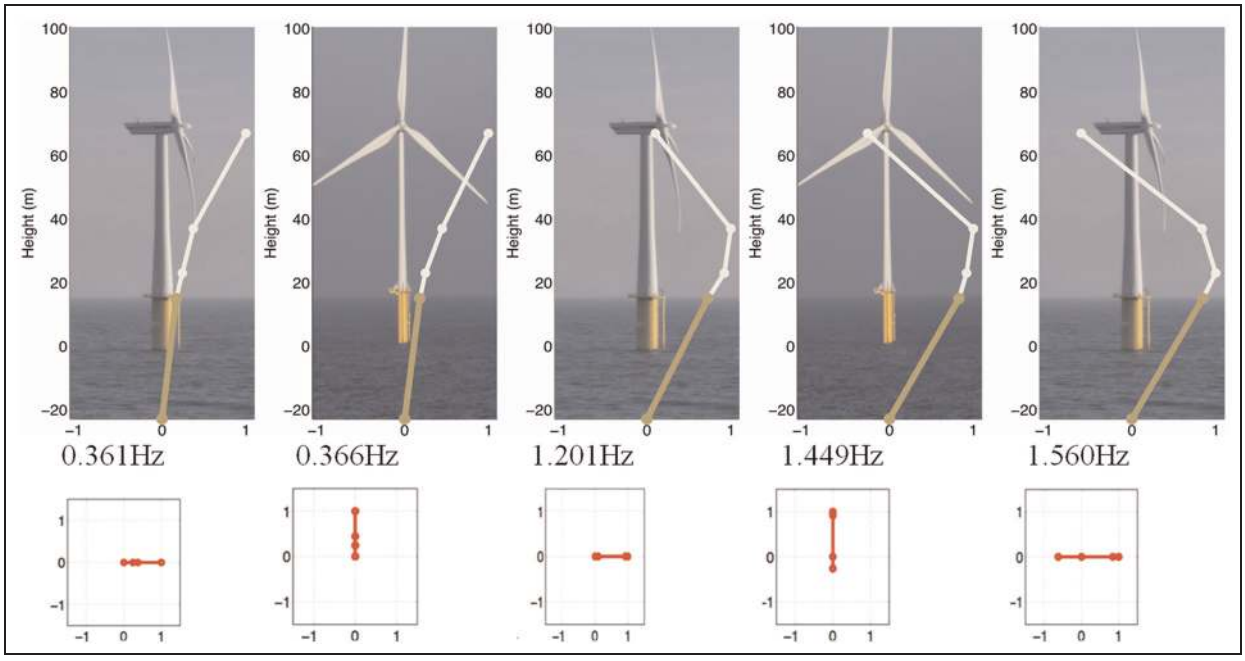

Figure 8. Five dominant identified mode shapes identified during the monitoring campaign.

modes. The classification result of the mode around 0.37 Hz (first SS mode) and 1.2 Hz (second FA mode) was slightly lowered due to a low fraction of mode shapes that have an MPC larger than 80%. As a result, the mode around 0.37 Hz, although physical, is no longer positively classified in this data set.

When applying the proposed method to the 2016 data sets of 10 min of data, most of the times five clusters were retained by the above-presented method using all classification variables. These five clusters correspond with the five dominant vibration modes that were well excited and identified while the wind turbine was in parked conditions. The mode shapes are shown in Figure 8. The first mode is the first FA bending mode (FA1). The second mode is the first SS bending mode (SS1). These modes are characterized by a lot of motion at the nacelle level. Next, a mode with a second FA bending mode behavior in the tower and almost no motion at nacelle level (FA2) is identified. This mode is in fact a coupled blade mode inducing some vibrations in tower and foundation in the FA direction. The last two modes also show a second bending mode behavior in the tower but with a small motion of the nacelle, respectively, in the SS (SS2N) and FA (FA2N) directions. These modes are the actual second bending modes of tower and foundation, respectively, in the SS and FA directions.

It can be concluded that the implemented algorithm seems to be an efficient approach for the classification of the identified clusters and thus can be considered as a valuable tool to be used in automatic identification and continuous monitoring. Other variables can be defined and used in the algorithm, for example, variables based on pole zero pairs and pole zero correlations.[13,21] Note also that in Table 2, the mean MAC values of all clusters are high; therefore, considering this information in the first or second clustering step would probably not have altered the results a lot.

Tracking of natural frequencies, mode shapes, and modal damping values (Step 3)

In the last step, the different physical modes are tracked over time. Since the natural frequencies and damping ratios of the modes may change due to changes in the operating conditions, it is not always straightforward to determine which identified modes from two subsequent data sets correspond to the same physical mode. Furthermore, it can happen that two modes cross each other in terms of natural frequency or damping ratio or even that the estimation algorithm returns a single mode at the moment of crossing, masking the other mode and seriously hampering the tracking process. In the case of the wind turbine, this is observed with the closely spaced first FA mode and first SS mode. Due to small asymmetries in the structure or soil conditions, these modes can have crossing frequencies due to changing yaw angles. In the presented method, the mode shape information in the form of the MAC is applied for mode tracking.

Initially, the modes of interest for the tracking are selected from the reference model obtained from an analysis of the first data sets. Mode tracking over the consecutive instants is done from a group composed by all the physical cluster mean estimates that have a natural frequency that does not differ more than 5% from the reference value. The cluster with the highest MAC value is selected and is only accepted if the MAC ratio is higher than 0.8. This approach makes it possible to track estimates of the same physical mode and allows possible frequency shifts lower than 5%, motivated by the different ambient and operating conditions or hypothetical damages. The reference modal parameters (natural frequencies, modal damping ratios, and mode shapes) used in this case are the ones presented in Figure 8.

Figure 9 illustrates the different mode shapes identified in the 2016 successive data sets. It can be seen that the mode shapes are very coherent over the different data sets, indicating that the adopted methodology is clearly able to track the different physical modes. Small differences can be attributed to, for example, small errors on the yaw angle used for the coordinate transformation or small asymmetries in the foundation structure and soil conditions.

Monitoring results

This section presents the obtained results using the presented continuous and automated monitoring approach using two different state-of-the-art OMA algorithms in Step 2, respectively, the p-LSCF and SSI-COV method. Figure 10 presents the evolution of the natural frequencies and the modal damping values of the five tracked modes during the monitoring period. The methodology has been able to successfully identify the closely spaced FA and SS modes, even when the frequencies cross each other. The methodology also successfully managed to capture the small daily variation on the resonance frequencies of the highest three modes. These changes can be attributed to the tidal effect. Figure 11 shows the evolution of the resonance frequency of the fourth monitored mode with the tidal level during 1 day. The lowest two modes seem to be less sensitive to this effect. This can be understood due to the fact that the highest three modes, all showing a second bending mode behavior, have a higher relative motion

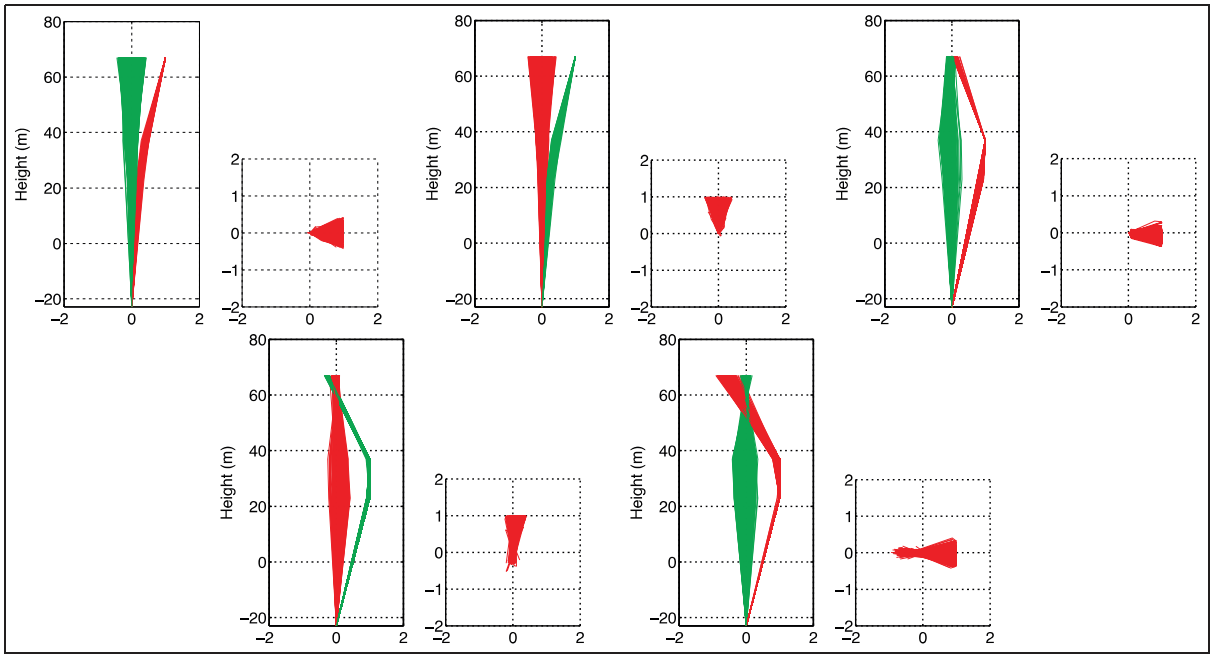

Figure 9. Evolution of the mode shapes of the five dominant modes during monitoring period: FA-direction (red lines) SS-direction (green lines), top views (right figures); from top left to bottom right: FA1, SS1, FA2, SS2N, and FA2N.
FA: fore-aft; SS: side–side.

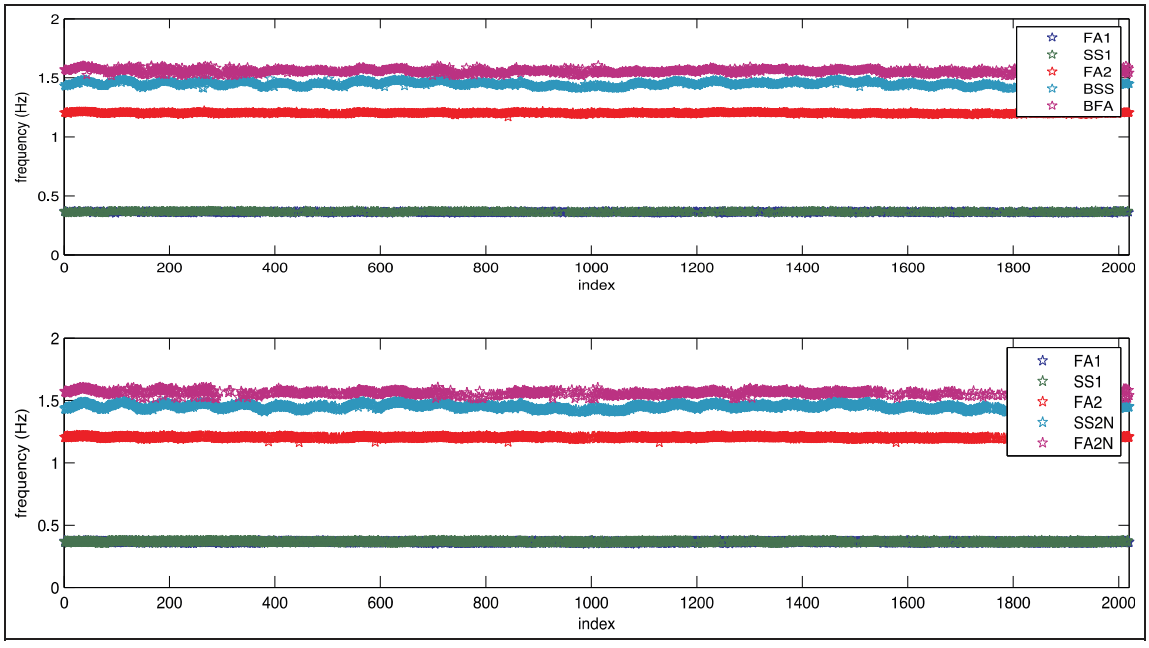

Figure 10. Evolution of frequencies of the five dominant modes during monitoring period using the p-LSCF estimator (top) using the SSI approach (bottom).
p-LSCF: poly-reference least squares complex frequency-domain estimator; SSI: stochastic subspace identification; FA: fore-aft.

at the water level in comparison with the first FA and SS bending modes. The same reasoning can be followed to justify why the frequencies of the second-order bending modes of this structure are more sensitive to scour as referred in the introduction. These modes have a larger relative motion at the mudline in comparison

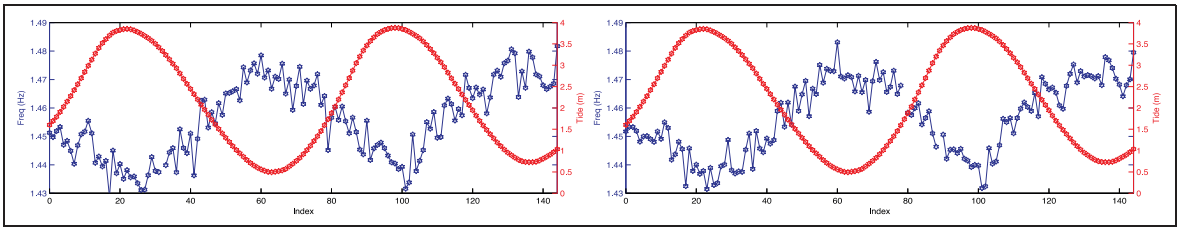

Figure 11. Variation during 24 h of the identified frequencies of mode 4 (FA2N) (blue) and the tidal level (red) using the p-LSCF estimator (left) using the SSI-COV method (right).
FA: fore-aft; p-LSCF: poly-reference least squares complex frequency-domain estimator; SSI-COV: covariance-driven stochastic subspace identification.

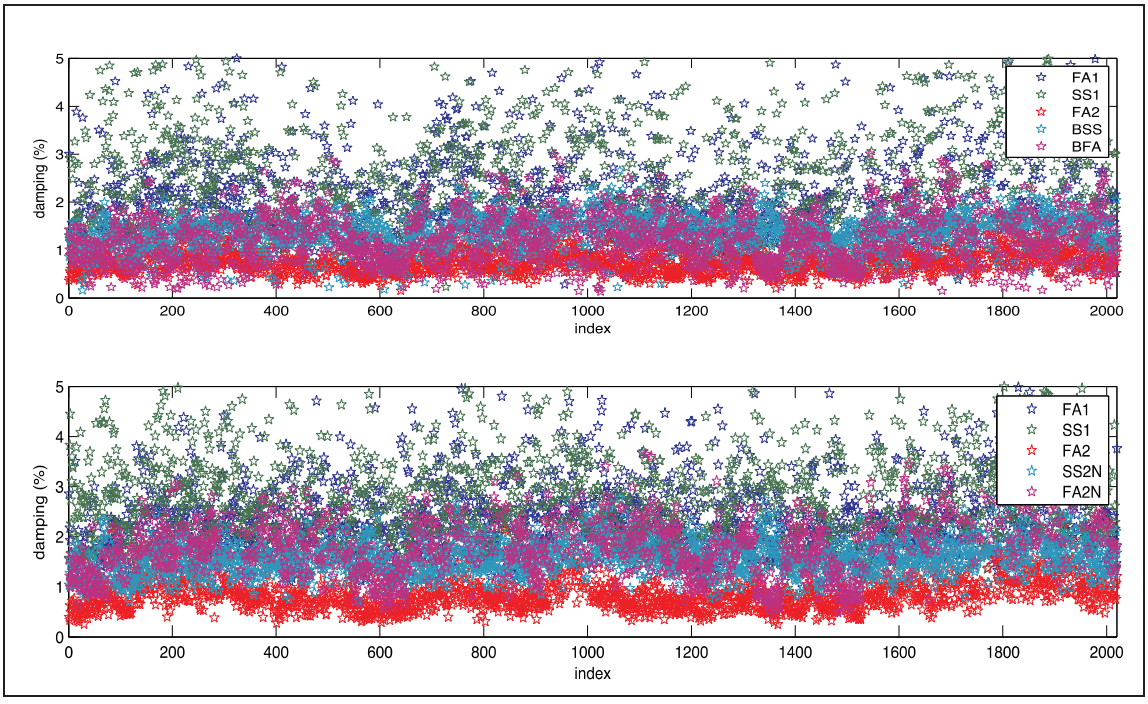

Figure 12. Evolution of damping values of the five dominant modes during monitoring period using the p-LSCF estimator (top) using the SSI approach (bottom).
p-LSCF: poly-reference least squares complex frequency-domain estimator; SSI-COV: covariance-driven stochastic subspace identification; FA: fore-aft.

with the first bending modes. Obviously, tracking the frequencies of the second-order bending modes will be of great interest if one wants to monitor scour. The accuracy at which the method is able to track changes due to the tidal level is promising toward using the approach to monitor changes in soil conditions.

The variation in the modal damping ratios of all the tracked modes is represented in Figure 12. It can be observed that the values for the three higher modes are reasonably coherent (taking into account that the estimates of the modal damping ratios always present some uncertainties), while the ones associated with the two lower modes present a higher scatter. This can be explained by the fact that identifying two closely spaced modes always increases the uncertainty, especially on the damping values. Also, the fact that only 10 min of data are used affects more significantly the quality of the estimates of the lower modes. However, a part of this high scatter can also be attributed to the high dependence of the damping of these modes with different operational and ambient parameters, for example, the wind speed. Figure 13 gives the complete overview of the damping values of all modes as a function of the wind speed obtained during the 14 days of monitoring. The red lines indicate the linear fit through all measured data points. These lines give a good first

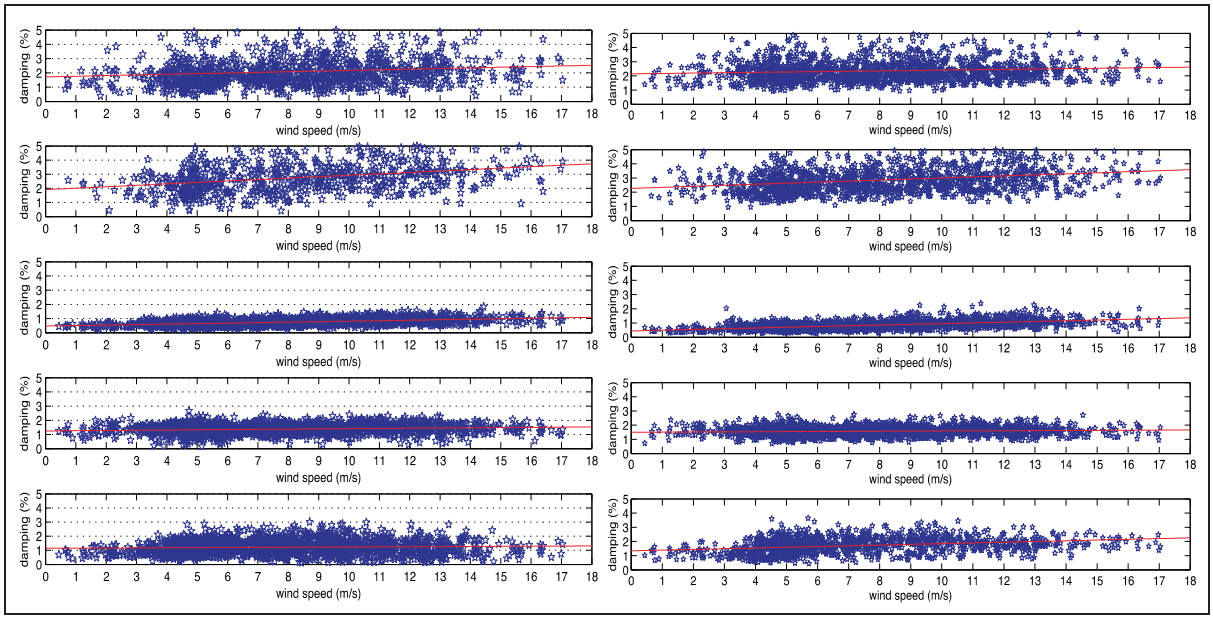

Figure 13. Damping values of the five dominant modes (from top to down: mode 1 (FA1), mode 2 (SS1), mode 3 (FA2), mode 4 (FA2N), and mode 5 (SS2N)) in function of wind speed using p-LSCF (left) and SSI (right)
FA: fore-aft; SS: side–side; p-LSCF: poly-reference least squares complex frequency-domain estimator; SSI: stochastic subspace identification.

indication about the relation between the damping values and the wind speeds for the different modes.

Table 3 synthesizes the results of the continuous monitoring routines in the processing of 14 days of data. In the second column, the success rate of the identification of the five dominant modes is quantified. The lowest success rate can be found for the first SS bending mode (SS1). This could be expected, as this mode is most of the time only weakly excited, thus difficult to identify. The success rate of the highly excited first FA mode (FA1) is higher. It can also be concluded that the identification of the closely spaced first FA mode and SS mode is difficult, but feasible. During this monitoring period, the SSI-COV approach resulted in a slightly higher success rate for the first two modes. The other three modes, FA2, SS2N, and FA2N, present high success rates for both methods. Columns 3–6 present the mean values and the SDs (std) of the natural frequencies (freq) and damping values (damp) within the monitoring period. The higher SDs on the frequencies of the two higher modes show that the influence of ambient conditions, such as the tidal effect, is higher on these modes. With regard to the damping values, a higher SD on the first two modes is observed, motivated by the reasons already discussed above. The SSI-COV approach identifies slightly higher damping values than the p-LSCF approach for all modes. The mean values of the MAC coefficients are high (higher than 0.9), which means that the mode shapes are not very sensitive to the ambient conditions and that the adopted identification procedure derived always high-quality estimates. This also validates the MAC-driven tracking algorithm.

Conclusion

This article presents a state-of-the art long-term dynamic monitoring solution for offshore wind turbines. The described processing algorithms include automatic pre-processing and online identification of the wind turbine dynamic parameters. The proposed method proved to be very efficient in the identification and tracking of the wind turbine five most dominant modes in parked conditions. The two tested identification algorithms, p-LSCF and SSI-COV, were capable of identifying the modes of interest even adopting short data sets of 10 min. In this monitoring campaign, the SSI-COV approach yielded a higher success rate for the closely spaced first FA and SS modes. The SSI-COV approach also resulted in slightly higher damping values for all modes.

The results obtained during 14 days, which involved the analysis of 2016 data sets, showed the ability of the proposed approach for automated monitoring. The method achieved a high accuracy of the estimates, enabling the detection of small variations in the frequencies and modal damping values due to fluctuations in the operational or ambient conditions.

The main advantage of the adopted processing methodologies can be found in the continuous monitoring of

Table 3. Results of the continuous monitoring using the p-LSCF estimator (left) and the SSI-COV approach (right).

Mode	Success rate (%)	Mean freq. (Hz)	Std freq. (Hz)	Mean damp. (%)	Std damp. (%)	Mean MAC	Min. MAC	Mode	Success rate (%)	Mean freq. (Hz)	Std freq. (Hz)	Mean damp. (%)	Std damp. (%)	Mean MAC	Min. MAC
FA1	72	0.361	0.004	1.86	0.85	0.91	0.80	FA1	84	0.362	0.003	2.12	0.85	0.91	0.80
SS1	50	0.366	0.005	2.49	0.97	0.90	0.80	SS1	62	0.366	0.004	2.66	1.38	0.90	0.80
FA2	97	1.201	0.006	0.72	0.22	0.98	0.80	FA2	97	1.201	0.006	0.79	0.30	0.98	0.80
SS2N	94	1.449	0.018	1.38	0.33	0.98	0.81	SS2N	94	1.449	0.018	1.53	0.33	0.98	0.81
FA2N	88	1.560	0.016	1.14	0.49	0.95	0.80	FA2N	85	1.562	0.017	1.57	0.55	0.95	0.80

p-LSCF: poly-reference least squares complex frequency-domain estimator; SSI-COV: covariance-driven stochastic subspace identification; MAC: modal assurance criterion; FA: fore-aft; SS: side–side.

the resonance frequencies (and damping ratios) of several structural modes over a long period using ambient excitation only instead of commonly used periodically start–stop events. The automated OMA thus allows identification over the full range of operational conditions rather during a very particular event, that is, a rotor stop. These long-term data will allow distinguishing the operational and environmental variability of the resonance frequencies of the turbine form the structural changes using regression models or principal component analysis (PCA).

Future studies will be conducted to understand and eliminate the effect of the different operational and ambient conditions on the identified parameters. This will be required in order to exploit the use of these parameters in the identification of changes in the dynamic behavior and structural integrity of the offshore wind turbine. The next challenge will also be to evaluate the proposed processing methodology on the data sets obtained while the wind turbine is rotating at rated speed.

Acknowledgements

This research has been performed in the framework of the Offshore Wind Infrastructure Project (http://www.owi-lab.be) and the IWT SBO project Optiwind. The authors gratefully thank the people of Belwind NV for their support before, during and after the installation of the measurement equipment.

Funding

The authors acknowledge the Fund for Scientific Research—Flanders (FWO).

References

1. Van Der Tempel J. *Design of support structures for offshore wind turbines*. PhD Thesis, TU Delft, Delft, 2006.
2. Maritime Research Institute Netherlands (MARIN). http://www.marin.nl/web/Events/Events-2010/Presentations-Offshore-Wind-Seminar-2010.htm (2010).
3. Zaaijer MB. *Tripod support structure—pre-design and natural frequency assessment for the 6 MW DOWEC*. Doc. no. 63, TU Delft, Delft, 14 May 2002.
4. Chauhan S, Tcherniak D, Basurko J, et al. Operational modal analysis of operating wind turbines: application to measured data. In: Proulx T (ed.) *Rotating machinery, structural health monitoring, shock and vibration* (proceedings of the society for experimental mechanics series 8), vol. 5. Berlin, Heidelberg: Springer, pp. 65–81.
5. Carne TG and James GH. The inception of OMA in the development of modal testing technology for wind turbines. *Mech Syst Signal Pr* 2010; 24, 1213–1226.
6. Hermans L and Van Der Auweraer H. Modal testing and analysis of structures under operational conditions: industrial applications. *Mech Syst Signal Pr* 1999; 13(2): 193–216.
7. Brincker R, Zhang L and Andersen P. Modal identification of output only systems using frequency domain decomposition. *Smar Mat St* 2001; 10: 441–445.

8. Cauberghe B. *Applied frequency-domain system identification in the field of experimental and operational modal analysis*. PhD Thesis, Vrije Universiteit Brussel, Brussels, 2004.
9. Devriendt C and Guillaume P. Identification of modal parameters from transmissibility measurements. *Journal of Sound and Vibration* 2008; 314(1–2): 343–356.
10. El-Kafafy M, Devriendt C, De Sitter G, et al. Damping estimation of offshore wind turbines using state-of-the art operational modal analysis techniques. In: *International conference on noise and vibration engineering*, Leuven, 17–19 September 2012.
11. Cauberghe B, Guillaume P, Verboven P, et al. The influence of the parameter constraint on the stability of the poles and the discrimination capabilities of the stabilisation diagrams. *Mech Syst Signal Pr* 2005; 19(5): 989–1014.
12. Guillaume P, Verboven P, Vanlanduit S, et al. A poly-reference implementation of the least-squares complex frequency domain-estimator. In: *Proceedings of the IMAC XXI*, Kissimmee, FL, 3–6 February 2003.
13. Verboven P, Parloo E, Guillaume P, et al. Autonomous structural health monitoring. Part 1: modal parameter estimation and tracking. *Mech Syst Signal Pr* 2002; 16(4): 637–657.
14. Reynders E, Houbrechts J and De Roeck G. Fully automated (operational) modal analysis. *Mech Syst Signal Pr* 2012; 29: 228–250.
15. Scionti M, Lanslots J, Goethals I, et al. Tools to improve detection of structural changes from in-flight flutter data. In: *Proceedings of eighth international conference on recent advances in structural dynamics*, Southampton, 13–16 July 2003.
16. Hair J, Anderson R, Tatham R, et al. *Multivariate data analysis*. Upper Saddle River, NJ: Prentice Hall, 1998.
17. Goethals I, Vanluyten B and De Moor B. Reliable spurious mode rejection using self-learning algorithms. In: *Proceedings of ISMA, international conference on noise and vibration engineering*, Leuven, 20–22 September 2004.
18. Carden EP and Brownjohn JMW. Fuzzy clustering of stability diagrams for vibration-based structural health monitoring. *Comput-Aided Civ Inf* 2008; 23(5): 360–372.
19. Magalhães F, Cunha A and Caetano E. On line automatic identification of the modal parameters of a long span arch bridge. *Mech Syst Signal Pr* 2009; 23(2): 316–329.
20. Verboven P, Guillaume P, Cauberghe B, et al. Stabilization charts and uncertainty bounds for frequency-domain linear least squares estimators. In: *Proceedings of IMAC 21, international modal analysis conference*, Kissimmee, FL, 3–6 February 2003.
21. Vanlanduit S, Verboven P, Guillaume P, et al. An automatic frequency domain modal parameter estimation algorithm. *J Sound Vib* 2003; 265(3): 647–661.
22. Peeters B and De Roeck G. Reference based stochastic subspace identification in civil engineering. *Inverse Probl Eng* 2000; 8(1): 47–74.
23. Magalhães F, Cunha A, Caetano E, et al. Damping estimation using free decays and ambient vibration tests. *Mech Syst Signal Pr* 2010; 24(5): 1274–1290.
24. Bendat J and Piersol A. *Engineering applications of correlation and spectral analysis*. New York: John Wiley & Sons, 1980.
25. Devriendt C, Jan Jordaens P, De Sitter G, et al. Damping estimation of an offshore wind turbine on a monopile foundation. In: *EWEA 2012*, Copenhagen, 16–19 April 2012.
26. Devriendt C, Jan Jordaens P, De Sitter G, et al. Damping estimation of an offshore wind turbine on a monopile foundation. *IET Renewable Power Generation* 2013; 7(4): 401–412.
27. Verboven P, Cauberghe B, Parloo S, et al. User-assisting tools for a fast frequency-domain modal parameter estimation method. *Mech Syst Signal Pr* 2004; 18(4): 759–780.
28. Maia NMM and Silva JMM. *Theoretical and experimental modal analysis*. Baldock: Research Studies Press Ltd, 1997.